

# Power-law Cosmology in Weyl type $f(Q, T)$ Gravity

**P.K. Sahoo**

Department of Mathematics  
Birla Institute of Technology and Science-Pilani,  
Hyderabad Campus, Hyderabad 500078, India

*pk\_sahoo@hyderabad.bits-pilani.ac.in*



# Topic Outlines

Overview of Weyl geometry

Weyl type  $f(Q, T)$  gravity and its formalism

Solutions to the Field Equations

Best fit values of model parameters from observation

Statefinder diagnostics

$Om$  diagnostic

Conclusion



# Overview of Weyl geometry

- ▶ Weyl introduced in 1918 a generalization of the Riemann geometry called Weyl geometry, to unify theory of gravity and electromagnetism.



# Overview of Weyl geometry

- ▶ Weyl introduced in 1918 a generalization of the Riemann geometry called Weyl geometry, to unify theory of gravity and electromagnetism.
- ▶ The idea was to allow both the orientation and the length of vectors to vary under parallel transport, while in Riemann geometry only the variation of the orientation is allowed.



# Overview of Weyl geometry

- ▶ Weyl introduced in 1918 a generalization of the Riemann geometry called Weyl geometry, to unify theory of gravity and electromagnetism.
- ▶ The idea was to allow both the orientation and the length of vectors to vary under parallel transport, while in Riemann geometry only the variation of the orientation is allowed.
- ▶ To describe mathematically these two simultaneous changes, Weyl proposed the introduction of a new vector field  $w_\mu$ , which, together with the metric tensor  $g_{\mu\nu}$ , represents the fundamental fields of the Weyl geometry.



- ▶ **Example I:-** If in a Weyl space a vector of length  $l$  is carried along an infinitesimal path  $\delta x^\mu$  by parallel transport, the variation in its length  $\delta l$  is given by the expression  $\delta l = l w_\mu \delta x^\mu$ .



- ▶ **Example I:-** If in a Weyl space a vector of length  $l$  is carried along an infinitesimal path  $\delta x^\mu$  by parallel transport, the variation in its length  $\delta l$  is given by the expression  $\delta l = l w_\mu \delta x^\mu$ .
- ▶ **Example II:-** After the parallel transport of a vector around a small closed loop of area  $\delta s^{\mu\nu}$ , the variation of the length of the vector is given by the expression  $\delta l = l W_{\mu\nu} \delta s^{\mu\nu}$ , where  $W_{\mu\nu} = \nabla_\nu w_\mu - \nabla_\mu w_\nu$ .



- ▶ **Example I:-** If in a Weyl space a vector of length  $l$  is carried along an infinitesimal path  $\delta x^\mu$  by parallel transport, the variation in its length  $\delta l$  is given by the expression  $\delta l = l w_\mu \delta x^\mu$ .
- ▶ **Example II:-** After the parallel transport of a vector around a small closed loop of area  $\delta S^{\mu\nu}$ , the variation of the length of the vector is given by the expression  $\delta l = l W_{\mu\nu} \delta S^{\mu\nu}$ , where  $W_{\mu\nu} = \nabla_\nu w_\mu - \nabla_\mu w_\nu$ .
- ▶ Another important property of the Weyl geometry is the existence of the semi-metric connection,

$$\tilde{\Gamma}_{\mu\nu}^\lambda = \Gamma_{\mu\nu}^\lambda + g_{\mu\nu} w^\lambda - \delta_\mu^\lambda w_\nu - \delta_\nu^\lambda w_\mu \quad (1)$$

where  $\Gamma_{\mu\nu}^\lambda$  is the Christoffel symbol constructed with respect to the metric  $g_{\mu\nu}$ .



- In Riemannian geometry, the Levi-Civita connection is compatible with the metric, i.e.,  $\nabla_\lambda g_{\mu\nu} = 0$ . This is not the case for the semi-metric connection in Weyl geometry, hence

$$Q_{\lambda\mu\nu} = \nabla_\lambda g_{\mu\nu} = \partial_\lambda g_{\mu\nu} - \tilde{\Gamma}_{\lambda\mu}^\rho g_{\rho\nu} - \tilde{\Gamma}_{\lambda\nu}^\rho g_{\rho\mu} \quad (2)$$



- ▶ In Riemannian geometry, the Levi-Civita connection is compatible with the metric, i.e.,  $\nabla_\lambda g_{\mu\nu} = 0$ . This is not the case for the semi-metric connection in Weyl geometry, hence

$$Q_{\lambda\mu\nu} = \nabla_\lambda g_{\mu\nu} = \partial_\lambda g_{\mu\nu} - \tilde{\Gamma}_{\lambda\mu}^\rho g_{\rho\nu} - \tilde{\Gamma}_{\lambda\nu}^\rho g_{\rho\mu} \quad (2)$$

- ▶ The non-metricity tensor in Weyl geometry is obtained as

$$Q_{\lambda\mu\nu} = 2w_\lambda g_{\mu\nu}, \quad w_\lambda \neq 0. \quad (3)$$



## Weyl type $f(Q, T)$ gravity

- ▶ In the context of proper Weyl geometry, we will discuss the cosmological model based on the recently proposed  $f(Q, T)$  gravity by Yixin Xu et al. <sup>1</sup>.
- ▶ The non-metricity  $Q_{\mu\nu\lambda}$  of the space-time was expressed in its standard Weyl form; therefore, it is fully determined by a vector field  $w_\mu$ .

---

<sup>1</sup>Xu Y. et al., Eur. Phys. J. C, **80**, 449, (2020)



## Weyl type $f(Q, T)$ gravity

- ▶ In the context of proper Weyl geometry, we will discuss the cosmological model based on the recently proposed  $f(Q, T)$  gravity by Yixin Xu et al. <sup>1</sup>.
- ▶ The non-metricity  $Q_{\mu\nu\lambda}$  of the space-time was expressed in its standard Weyl form; therefore, it is fully determined by a vector field  $w_\mu$ .
- ▶ The field equations of the theory have been obtained under the assumption of the vanishing of the total scalar curvature, a condition which was added into the gravitational action via a Lagrange multiplier  $\lambda$ .

---

<sup>1</sup>Xu Y. et al., Eur. Phys. J. C, **80**, 449, (2020)



## Weyl type $f(Q, T)$ gravity

- ▶ In the context of proper Weyl geometry, we will discuss the cosmological model based on the recently proposed  $f(Q, T)$  gravity by Yixin Xu et al. <sup>1</sup>.
- ▶ The non-metricity  $Q_{\mu\nu\lambda}$  of the space-time was expressed in its standard Weyl form; therefore, it is fully determined by a vector field  $w_\mu$ .
- ▶ The field equations of the theory have been obtained under the assumption of the vanishing of the total scalar curvature, a condition which was added into the gravitational action via a Lagrange multiplier  $\lambda$ .

---

<sup>1</sup>Xu Y. et al., Eur. Phys. J. C, **80**, 449, (2020)



- ▶ The Weyl type  $f(Q, T)$  gravity has been found to be an alternate and effective way of describing accelerated and decelerated phases of the universe.



- ▶ The Weyl type  $f(Q, T)$  gravity has been found to be an alternate and effective way of describing accelerated and decelerated phases of the universe.
- ▶ Studying variety of functional forms and model parameters, Weyl type  $f(Q, T)$  could provide a strong alternative to the  $\Lambda$ CDM, especially giving the late-time de sitter phase generated by Weyl geometry.



## formalism

- ▶ The action in Weyl type  $f(Q, T)$  gravity is given as <sup>2</sup>

$$S = \int d^4x \sqrt{-g} [\kappa^2 f(Q, T) - \frac{1}{4} W_{\nu\mu} W^{\nu\mu} - \frac{1}{2} m^2 w_\nu w^\nu + \lambda \tilde{R} + \mathcal{L}_m] \quad (4)$$

where  $\tilde{R} = (R + 6 \nabla_\alpha w^\alpha - 6 w_\alpha w^\alpha)$ ,  $\kappa = \frac{1}{16\pi G}$ ,  $m$  represents the mass of the particle associated to the vector field  $w_\mu$ ,  $f(Q, T)$  is an arbitrary function of the nonmetricity  $Q$  and the trace of energy momentum tensor  $T$ . The second and third terms in the action are the ordinary kinetic term and mass term of the vector field, respectively.  $W_{\nu\mu} = \nabla_\mu w_\nu - \nabla_\nu w_\mu$  and  $\mathcal{L}_m$  is the matter Lagrangian density.

---

<sup>2</sup>Xu Y. et al., Eur. Phys. J. C, **80**, 449, (2020)



- ▶ Variation of the gravitational action in Eq.(4) with to the metric tensor gives us the following generalized gravitational field equation:

$$\begin{aligned}
 \frac{1}{2} (T_{\nu\mu} + S_{\nu\mu}) - \kappa^2 f_T (T_{\nu\mu} + \Theta_{\nu\mu}) &= -\frac{\kappa^2}{2} g_{\nu\mu} \\
 - 6\kappa^2 f_Q w_\nu w_\mu + \lambda (R_{\nu\mu} - 6 w_\nu w_\mu + 3 g_{\nu\mu} \nabla_\rho w^\rho) \\
 + 3 g_{\nu\mu} w^\rho \nabla_\rho \lambda - 6 w_{(\nu} \nabla_{\mu)} \lambda + g_{\nu\mu} \square \lambda - \nabla_\nu \nabla_\mu \lambda. & \quad (5)
 \end{aligned}$$



- ▶ We consider that the universe is described by the spatially flat FLRW line element

$$ds^2 = -dt^2 + a^2(t)[dx^2 + dy^2 + dz^2]. \quad (6)$$

Where,  $a(t)$  is the scale factor



- ▶ We consider that the universe is described by the spatially flat FLRW line element

$$ds^2 = -dt^2 + a^2(t)[dx^2 + dy^2 + dz^2]. \quad (6)$$

Where,  $a(t)$  is the scale factor

- ▶ Because of spatial symmetry, the vector field is chosen in the form of

$$w_\nu = (\psi(t), 0, 0, 0) \quad (7)$$



- ▶ We consider that the universe is described by the spatially flat FLRW line element

$$ds^2 = -dt^2 + a^2(t)[dx^2 + dy^2 + dz^2]. \quad (6)$$

Where,  $a(t)$  is the scale factor

- ▶ Because of spatial symmetry, the vector field is chosen in the form of

$$w_\nu = (\psi(t), 0, 0, 0) \quad (7)$$

- ▶ The trace of the nonmetricity  $Q$  for the FLRW metric (6) takes the form below

$$Q = -6w^2 = 6\psi^2(t), \quad (8)$$

where  $w^2 = w_\mu w^\mu = -\psi^2(t)$ .



- ▶ From Eq. (5) and (6) the generalized Friedmann equation read as

$$\kappa^2 f_T (\rho + p) + \frac{1}{2}\rho = \frac{\kappa^2}{2}f - \left(6\kappa^2 f_Q + \frac{1}{4}m^2\right)\psi^2 - 3\lambda(\psi^2 - H^2) - 3\dot{\lambda}(\psi - H), \quad (9)$$

$$-\frac{1}{2}p = \frac{\kappa^2}{2}f + \frac{m^2\psi^2}{4} + \lambda(3\psi^2 + 3H^2 + 2\dot{H}) + (3\psi + 2H)\dot{\lambda} + \ddot{\lambda}. \quad (10)$$

where dot( $\cdot$ ) represents the derivative with respect to time.



- ▶ Now, we consider the functional form  $f(Q, T) = \alpha Q + \frac{\beta}{6\kappa^2} T$ , where  $\alpha$  and  $\beta$  are model parameters. It is worth mentioning that  $\beta = 0$  and  $\alpha = -1$  corresponds to the  $f(Q, T) = -Q$  i.e. a case of the successful theory of General Relativity (GR). Also,  $T = 0$ , the case of vacuum, the theory reduces to  $f(Q)$  gravity, that passes all Solar System tests, considered in the vacuum



- ▶ Now, we consider the functional form  $f(Q, T) = \alpha Q + \frac{\beta}{6\kappa^2} T$ , where  $\alpha$  and  $\beta$  are model parameters. It is worth mentioning that  $\beta = 0$  and  $\alpha = -1$  corresponds to the  $f(Q, T) = -Q$  i.e. a case of the successful theory of General Relativity (GR). Also,  $T = 0$ , the case of vacuum, the theory reduces to  $f(Q)$  gravity, that passes all Solar System tests, considered in the vacuum
- ▶ We study the model for the dust case, i.e.  $p = 0$ . Using this in Eq. (9) and (10), the obtained differential equation is,

$$A H^2 + B \dot{H} = 0 \quad (11)$$

where,

$$A = 36 \left( (12\beta + 18) \alpha + \left( \beta + \frac{3}{2} \right) M^2 + (12\beta + 18) \right) + (6\beta + 18)$$

and  $B = (6\beta + 12)$



# Solutions to the Field Equations

## The Hubble parameter and deceleration parameter

The obtained solution of differential equation given in (11) is,

$$H(t) = \frac{1}{k_1 t - c_1} \quad (12)$$

where,

$$k_1 = \frac{A}{B} = \left[ \frac{36(2\beta + 3)(\alpha + 1)}{(\beta + 2)} + \frac{(6\beta + 9)}{(\beta + 2)} M^2 + \frac{(\beta + 3)}{(\beta + 2)} \right]$$



# Solutions to the Field Equations

## The Hubble parameter and deceleration parameter

The obtained solution of differential equation given in (11) is,

$$H(t) = \frac{1}{k_1 t - c_1} \quad (12)$$

where,

$$k_1 = \frac{A}{B} = \left[ \frac{36(2\beta + 3)(\alpha + 1)}{(\beta + 2)} + \frac{(6\beta + 9)}{(\beta + 2)} M^2 + \frac{(\beta + 3)}{(\beta + 2)} \right]$$

Solving eq. (12), the expression of the scale factor is obtained as

$$a(t) = c_2 (k_1 t - c_1)^{\frac{1}{k_1}} \quad (13)$$

We shall write all cosmological parameter in term of redshift using the relation (taking  $a(t_0) = 1$ )

$$a(t) = \frac{1}{1 + z} \quad (14)$$



- ▶ The Hubble parameter and deceleration parameter in terms of redshift are,

$$H(z) = H_0(1 + z)^{k_1} \quad (15)$$

$$q(z) = (k_1 - 1) \quad (16)$$

Here, we have obtained the power-law as the solutions of the field equations

---

<sup>3</sup>Kumar S., MNRAS, **422**, 2532, (2012)

<sup>4</sup>Rani S. et al., JCAP, **03**, 031, (2015)



- ▶ The Hubble parameter and deceleration parameter in terms of redshift are,

$$H(z) = H_0(1 + z)^{k_1} \quad (15)$$

$$q(z) = (k_1 - 1) \quad (16)$$

Here, we have obtained the power-law as the solutions of the field equations

- ▶ Power-law cosmology is an interesting solution for dealing with some unusual challenges like flatness, horizon problem, etc. The power-law is well-motivated in literature. Kumar <sup>3</sup> used power-law with Hz and SNe Ia data to analyse cosmological parameters. Rani et al. <sup>4</sup> also examined the power-law cosmology with statefinder analysis.

---

<sup>3</sup>Kumar S., MNRAS, **422**, 2532, (2012)

<sup>4</sup>Rani S. et al., JCAP, **03**, 031, (2015)



# Best fit values of model parameters from observation

## Hz and SNe Ia Data sets

- ▶ To obtain the best fit values of these model parameters, we have used mainly two datasets namely, the Hubble datasets containing 57 data points and the Pantheon datasets containing 1048 datapoints. In this set of 57 Hubble data points, 31 points measured via the method of differential age (DA) and remaining 26 points through BAO and other methods <sup>5</sup>

---

<sup>5</sup>G. S. Sharov, V.O. Vasiliev, *Mathematical Modelling and Geometry* **6**, 1 (2018)

<sup>6</sup>D. M. Scolnic et al., *Astrophys. J.*, **859**, 101, (2018).



# Best fit values of model parameters from observation

## Hz and SNe Ia Data sets

- ▶ To obtain the best fit values of these model parameters, we have used mainly two datasets namely, the Hubble datasets containing 57 data points and the Pantheon datasets containing 1048 datapoints. In this set of 57 Hubble data points, 31 points measured via the method of differential age (DA) and remaining 26 points through BAO and other methods <sup>5</sup>
- ▶ Recently, the latest sample of supernovae of type Ia datasets are released containing 1048 data points. In this article, we have used this set of 1048 data points known as Pantheon datasets <sup>6</sup>.

---

<sup>5</sup>G. S. Sharov, V.O. Vasiliev, *Mathematical Modelling and Geometry* **6**, 1 (2018)

<sup>6</sup>D. M. Scolnic et al., *Astrophys. J.*, **859**, 101, (2018).



- ▶ The chi-square function is defined to find the mean values of the model parameters  $\alpha$  and  $\beta$ .

$$\chi_{Hubble}^2(\alpha, \beta) = \sum_{i=1}^{57} \frac{[H_i^{th}(\alpha, \beta, z_i) - H_i^{obs}(z_i)]^2}{\sigma^2(z_i)} \quad (17)$$

where  $H_i^{obs}$  denotes the observed value,  $H_i^{th}$  indicates the Hubble's theoretical value while the standard error in the observed value is denoted by  $\sigma(z_i)$ . We used error bars to represent 57 points of  $H(z)$  and compared our model with the well-accepted  $\Lambda$ CDM model in fig. 1(a). The bounds from our analysis are  $\alpha = -1.08448_{-0.00055}^{+0.00049}$  and  $\beta = 0.136_{-0.110}^{+0.056}$ .



- ▶ We use the most recent compilation of Supernovae pantheon samples to constrain the model parameters  $\alpha$  and  $\beta$ . The theoretical distance modulus is defined as

$$\mu^{th} = 5 \log_{10} \left( \frac{D_L H_0^{-1}}{Mpc} \right) + 25, \quad (18)$$

where we define

$$D_L = (1+z)c \int_0^z \frac{d\bar{z}}{H(\bar{z})}. \quad (19)$$

- ▶ The chi-square function according to our considered model is given as

$$\chi_{Pan}^2(\alpha, \beta) = \sum_{i=1}^{1048} \frac{[\mu_i^{th}(\alpha, \beta, z_i) - \mu_i^{obs}(z_i)]^2}{\sigma^2(z_i)} \quad (20)$$

where  $\sigma^2(z_i)$  is the standard error,  $\mu_i^{th} = m - M$  is the theoretical value with  $m$  and  $M$  are the apparent and absolute magnitudes respectively,  $\mu_i^{obs}$  is the observed values from data points.



- ▶ The best fit values of  $\alpha$  and  $\beta$  are obtained through pantheon samples as shown in triangle plot 3 with  $1 - \sigma$  and  $2 - \sigma$  confidence intervals. The obtained values are

$$\alpha = -1.09519^{+0.00060}_{-0.00068} \text{ and } \beta = 0.137^{+0.058}_{-0.100}$$



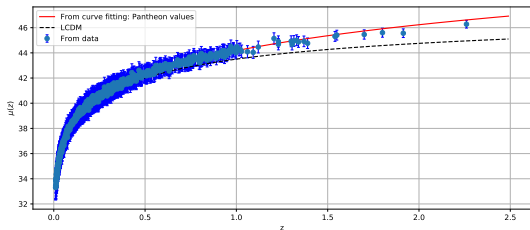
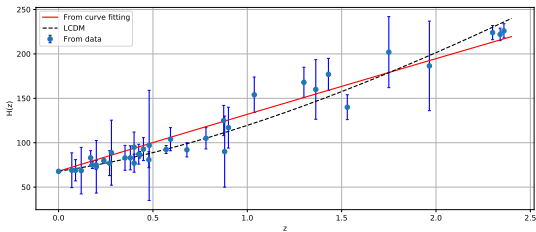


**Figure 1:** The plot shows the 57 points of  $H(z)$  datasets and 1048 points of SNe Ia (Blue dots) datasets with corresponding error bars. The plot shows nice fit of our model (Red line) to the observational datasets.  $\Lambda$ CDM model is also shown in black line for model comparison.



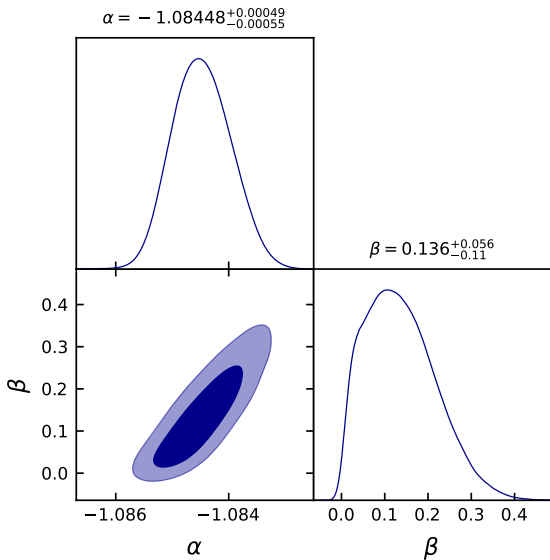


Figure 2: The figure shows the contour plot for the model parameters  $\alpha, \beta$  for the Hubble data at  $1 - \sigma, 2 - \sigma$  confidence level.



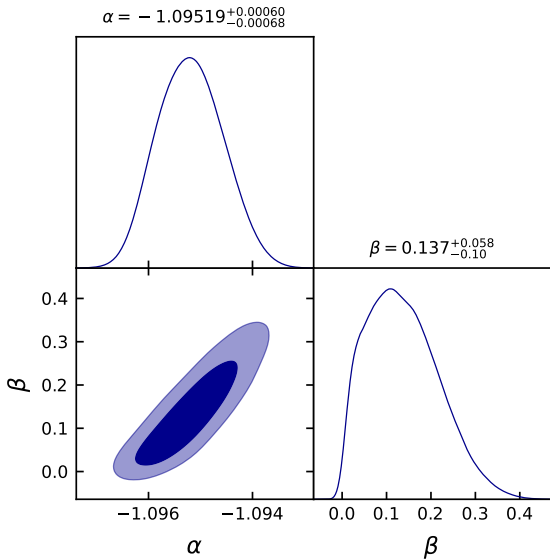


Figure 3: The figure shows the contour plot for the model parameters  $\alpha, \beta$  for the Pantheon data at  $1 - \sigma, 2 - \sigma$  confidence level.



## Statefinder diagnostics

- ▶ The problem of discriminating different dark energy models is now emergent. In order to solve this problem, a sensitive and robust diagnostic for dark energy is a must. For this purpose a diagnostic proposal that makes use of parameter pair  $r - s$ , the so-called "statefinder", was introduced by Sahni et al. <sup>7</sup>

---

<sup>7</sup> Sahni V. et al., JETP Lett., **77**, 201, (2003)



# Statefinder diagnostics

- ▶ The problem of discriminating different dark energy models is now emergent. In order to solve this problem, a sensitive and robust diagnostic for dark energy is a must. For this purpose a diagnostic proposal that makes use of parameter pair  $r - s$ , the so-called "statefinder", was introduced by Sahni et al. <sup>7</sup>
- ▶ It is defined with the help of well known geometrical parameters namely the Hubble parameter  $H = \frac{\dot{a}}{a}$  and the deceleration parameter  $q = -\frac{\ddot{a}}{aH^2}$ . The statefinder parameter pair  $r - s$  is defined as

$$r = \frac{\ddot{a}}{aH^3} \quad s = \frac{r - 1}{3(q - \frac{1}{2})}. \quad (21)$$

---

<sup>7</sup> Sahni V. et al., JETP Lett., **77**, 201, (2003)



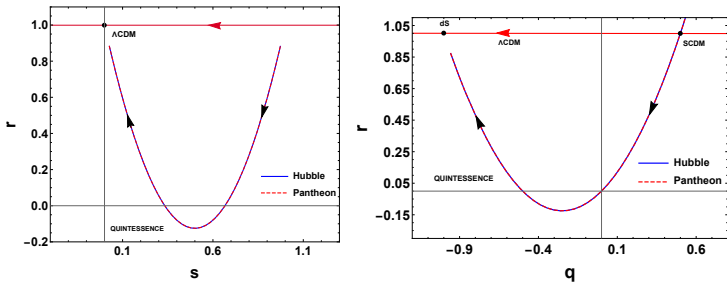


Figure 4: The evolution trajectories of the given model in  $s$ - $r$  and  $q$ - $r$  plane corresponding to the values of model parameters constrained by the Hubble and Pantheon datasets.



- ▶ The statefinder parameter  $s - r$  can be an admirable diagnostic for describing significant dark energy model characteristics. According to the trajectories in  $s - r$  plane, the point  $(0, 1)$  corresponds to the  $\Lambda$ CDM model, Chaplygin gas lie to the left of the  $\Lambda$ CDM model whereas quintessence lie to the right of the  $\Lambda$ CDM



- ▶ The statefinder parameter  $s - r$  can be an admirable diagnostic for describing significant dark energy model characteristics. According to the trajectories in  $s - r$  plane, the point  $(0, 1)$  corresponds to the  $\Lambda$ CDM model, Chaplygin gas lie to the left of the  $\Lambda$ CDM model whereas quintessence lie to the right of the  $\Lambda$ CDM
- ▶ In  $q - r$  figure, it is observed the point  $(q, r) = (0.5, 1)$  correspond to  $SCDM$  (i.e. matter dominated universe), with the de-sitter (dS) expansion pointing to  $(q, r) = (-1, 1)$  in the future. As a result, the statefinder diagnostics can successfully distinguish between various dark energy models



- ▶ The statefinder parameter  $s - r$  can be an admirable diagnostic for describing significant dark energy model characteristics. According to the trajectories in  $s - r$  plane, the point  $(0, 1)$  corresponds to the  $\Lambda$ CDM model, Chaplygin gas lie to the left of the  $\Lambda$ CDM model whereas quintessence lie to the right of the  $\Lambda$ CDM
- ▶ In  $q - r$  figure, it is observed the point  $(q, r) = (0.5, 1)$  correspond to  $SCDM$  (i.e. matter dominated universe), with the de-sitter (dS) expansion pointing to  $(q, r) = (-1, 1)$  in the future. As a result, the statefinder diagnostics can successfully distinguish between various dark energy models
- ▶ It is worth noting that in the obtained model, the  $\Lambda$ CDM statefinder pair  $(0, 1)$  and correspondingly the dS point  $(-1, 1)$  acts as an attractor. The constraints on statefinder from Hubble data and Pantheon data are obtained as  $r = -0.039_{-0.009}^{+0.009}$ ,  $s = 0.637_{-0.0075}^{+0.0075}$  and  $r = -0.105_{-0.011}^{+0.008}$ ,  $s = 0.434_{-0.012}^{+0.023}$  respectively.



## $Om$ diagnostic

- ▶ The  $Om$  diagnostic <sup>8,9</sup> is used to clarify various dark energy (DE) models by differentiating  $\Lambda$  CDM model. For spatially flat universe, the  $Om(z)$  diagnostic is defined as

$$Om(z) = \frac{\left(\frac{H(z)}{H_0}\right)^2 - 1}{(1+z)^3 - 1} \quad (22)$$

where,  $H_0$  is the Hubble constant.

---

<sup>8</sup> Sahni V., Shafieloo A., Starobinsky A.A., Phys. Rev. D, **78**, 103502, (2008)

<sup>9</sup> Shahalam M., Sami S. & Agarwal A., MNRAS, **448**, 2948, (2015)



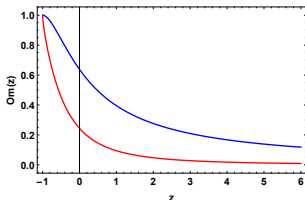
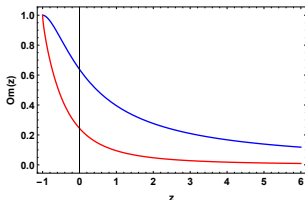


Figure 5: This figure shows the behavior of  $Om$  vs redshift  $z$  corresponding to the values of model parameters constrained by the Hubble and Pantheon datasets.





**Figure 5:** This figure shows the behavior of  $Om$  vs redshift  $z$  corresponding to the values of model parameters constrained by the Hubble and Pantheon datasets.

- ▶ According to the behavior of  $Om(z)$ , different dark energy models can be described. Phantom type i.e.  $\omega < -1$  corresponds to the positive slope of  $Om(z)$ , quintessence type  $\omega > -1$  corresponding to negative slope of  $Om(z)$ . The constant behavior of  $Om(z)$  depicts the  $\Lambda$ CDM model
- ▶ In Figure 5, the  $Om(z)$  has a negative slope, showing quintessence like behavior indicating the accelerated expansion.



# Conclusion

- ▶ In this discussion, we have seen the evolution of the Universe changes time to time depending upon the various matter source (in case of GR)
- ▶ We have considered the case of dust and obtained the solutions of the field equations. The Hubble parameter is found to be similar to the power-law form in redshift  $z$



# Conclusion

- ▶ In this discussion, we have seen the evolution of the Universe changes time to time depending upon the various matter source (in case of GR)
- ▶ We have considered the case of dust and obtained the solutions of the field equations. The Hubble parameter is found to be similar to the power-law form in redshift  $z$
- ▶ We have constrained our model to obtain the best fit ranges of the model parameters by using the Hubble datasets containing 57 data points and the Pantheon datasets containing 1048 data points



# Conclusion

- ▶ In this discussion, we have seen the evolution of the Universe changes time to time depending upon the various matter source (in case of GR)
- ▶ We have considered the case of dust and obtained the solutions of the field equations. The Hubble parameter is found to be similar to the power-law form in redshift  $z$
- ▶ We have constrained our model to obtain the best fit ranges of the model parameters by using the Hubble datasets containing 57 data points and the Pantheon datasets containing 1048 data points



## Conclusion

- ▶ According to the constraints values of  $\alpha$  and  $\beta$ , the deceleration parameter  $q$  is seen to be negative. However, it fails to provide redshift transition from deceleration to acceleration due to the constant value of the deceleration parameter



# Conclusion

- ▶ According to the constraints values of  $\alpha$  and  $\beta$ , the deceleration parameter  $q$  is seen to be negative. However, it fails to provide redshift transition from deceleration to acceleration due to the constant value of the deceleration parameter
- ▶ As a result, we used the statefinder diagnostics  $s - r$  and  $q - r$  and the  $Om$  diagnostic analysis for the model to study the nature of dark energy models



# Conclusion

- ▶ According to the constraints values of  $\alpha$  and  $\beta$ , the deceleration parameter  $q$  is seen to be negative. However, it fails to provide redshift transition from deceleration to acceleration due to the constant value of the deceleration parameter
- ▶ As a result, we used the statefinder diagnostics  $s - r$  and  $q - r$  and the  $Om$  diagnostic analysis for the model to study the nature of dark energy models
- ▶ Hence, the obtained model is proven to be helpful in describing the acceleration of present universe.



## References

- ▶ A.G. Riess et al., ApJ **116**, 1009 (1998).
- ▶ S. Perlmutter et al., ApJ **517**, 565 (1999).
- ▶ V. Sahni, A. Shafieloo, A.A. Starobinsky, Phys. Rev. D **78**, 103502 (2008).
- ▶ M. Shahalam, S. Sami, A. Agarwal, MNRAS **448**, 2948 (2015).
- ▶ S. Vagnozzi, Phys. Rev. D **102**, 023518 (2020).
- ▶ Valentino E. Di, Phys. Lett. B **761**, 242–246 (2016).



G.N. Gadbail, S. Arora, P.K. Sahoo, European Physical Journal  
Plus 136 (10), 1040 (2021).

**Thank you!**

